

Paramagnetic Semiconductors: Hybrid Molecular Materials Based on Ethyl- and Methyl-pyridinium-Substituted Verdazyl Radical Cations and the Ni(dmit)$_2$ Anion (dmit = 1,3-Dithiol-2-thione-4,5-dithiolate)

Kazuo Mukai,* Daisuke Shiba, Kenji Yoshida, Kyohei Mukai, Hiroyuki Hisatou, Keishi Ohara, Yuko Hosokoshi,[1] and Nagao Azuma

Department of Chemistry, Faculty of Science, Ehime University, Matsuyama 790-8577

[1]Department of Material Science, College of Integrated Arts and Sciences, Osaka Prefecture University, Sakai 599-8531

Received April 27, 2005; E-mail: mukai@chem.sci.ehime-u.ac.jp

Four kinds of 1:1 salts of 3-(4- and 3-alkyl-pyridinium)-1,5-diphenylverdazyl (alkyl = ethyl and methyl) radical cations with the Ni(dmit)$_2$ anion ([*p*-EtPyDV]$^+$[Ni(dmit)$_2$]$^-$ (**1**), [*m*-EtPyDV]$^+$[Ni(dmit)$_2$]$^-$ (**2**), [*p*-MePyDV]$^+$[Ni(dmit)$_2$]$^-$ (**3**), and [*m*-MePyDV]$^+$[Ni(dmit)$_2$]$^-$ (**4**)) have been prepared. The magnetic properties of salts **1**–**4** were discussed based on the results obtained by magnetic susceptibility and ESR measurements of **1**–**4** and the crystal structure analysis of **1**. The results of the crystal structure analysis of salt **1** indicate the dimer formation in Ni(dmit)$_2$ anion molecules, and the dimers are sandwiched between two verdazyl cations [*p*-EtPyDV]$^+$, indicating the formation of a magnetic linear tetramer in **1**. The magnetic susceptibility data for salt **1** have been fitted to a four-spin linear tetramer model using an end exchange interaction of $2J_1/k_B = -780$ K and a central interaction of $2J_2/k_B = -200$ K. The conductivity (σ) of salts **1**, **2**, **3**, and **4** at room temperature was $\sigma = 2.3 \times 10^{-5}$, 1.8×10^{-4}, 1.4×10^{-5}, and 5.4×10^{-6} S cm^{-1} with an activation energy of $E_A = 0.28$, 0.52, 0.21, and 0.33 eV, respectively. The 1:1 salts **1**–**4** are new molecular paramagnetic semiconductors.

Since the first molecular superconductor containing a transition-metal complex, (TTF)[M(dmit)$_2$]$_2$ (M = Ni and Pd, TTF = tetrathiafulvalene, and dmit = 1,3-dithiol-2-thione-4,5-dithiolato), was found by Brossard et al., extensive studies have been performed for assembled metal complexes, [Donor]-[M(dmit)$_2$]$_n$, exhibiting insulating, metallic and superconducting phases at low temperature under high pressure.[1–5] Two examples of magnetic semiconductors consisting of an open-shell radical cation donor and a metal complex anion acceptor have been reported for the 1:1 salt of [Ni(dmit)$_2$]$^-$ with *p*-EPYNN (*p*-*N*-ethylpyridinium α-nitronyl nitroxide) and Me$_3$N$^+$-TEMPO (=*N*,*N*,*N*-trimethyl(1-oxyl-2,2,6,6-tetramethylpiperidine-4-yl)ammonium) radical cations.[6,7]

It is well known that verdazyl radicals show high chemical and thermal stability and can be isolated as solvent-free pure radicals in crystalline states.[8–10] The magnetic properties of these verdazyl radical crystals have been studied recently, and several interesting magnetic properties such as ferromagnetism,[11,12] weak ferromagnetism,[13–15] antiferromagnetism,[16] spin-Peierls transition,[17–19] and spin frustration[20] have been found, indicating comparatively strong intermolecular spin–spin exchange interactions. Further, the intermolecular ferromagnetic (FM) interaction observed for these verdazyl radicals was of high probability because of a very strong spin polarization effect in these verdazyl radicals.[21]

Recently, the first two examples of molecular paramagnetic semiconductors consisting of verdazyl radical cations and metal complex anions have been reported for the Ni(dmit)$_2$ salts of 3-[4-(trialkylammonio)phenyl]-1,5-diphenyl-6-oxoverdazyl radical cations.[22,23] Further, the 1:1 and 1:2 salts of 3-(4- and 3-alkyl-pyridinium)-1,5-diphenylverdazyl radical cations (alkyl = ethyl and methyl) with the TCNQ anion were prepared, and the magnetic and conducting properties of these salts were studied.[24,25] The 1:2 salts were found to be genuine organic paramagnetic semiconductors. However, the examples of the molecular complexes between the open-shell radical cation and the electron acceptor anion are very limited. In the present work, we have prepared four kinds of 1:1 salts **1**–**4** of 3-(4- and 3-alkyl-pyridinium)-1,5-diphenylverdazyl (alkyl = ethyl and methyl) radical cations with the Ni(dmit)$_2$ anion (see Fig. 1), and studied the structural, magnetic, and conducting properties of these radical salts.

Development of molecular ferromagnets and superconductors is two challenging goals in material science, and many studies have been performed with great success in recent years. On the other hand, examples of magnetic conductors, where the superconducting (or metallic) state and antiferromagnetic (AFM) (or FM) order coexist in a system, are very limited because of the difficulty in molecular design of these complexes.[26–31] In particular, there have been no examples of molecular superconducting ferromagnets up to this time.

Experimental

Syntheses. The preparations of 3-(4-pyridyl)-1,5-diphenylverdazyl (*p*-PyDV) and 3-(3-pyridyl)-1,5-diphenylverdazyl (*m*-PyDV) radicals have been reported in a previous work.[20] The preparations of the iodide salts, 3-(4- and 3-alkyl-pyridinium)-1,5-diphenylverdazyl iodides (alkyl = ethyl and methyl), [*p*-EtPyDV]$^+$I$^-$ (**5**), [*m*-EtPyDV]$^+$I$^-$ (**6**), [*p*-MePyDV]$^+$I$^-$ (**7**), and [*m*-MePyDV]$^+$I$^-$ (**8**), have also been reported in previous papers.[24,25] Preparations of the

Published on the web December 9, 2005; DOI 10.1246/bcsj.78.2114

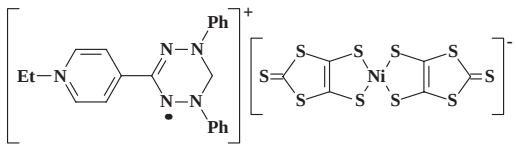

[*p*-EtPyDV]$^{+}$ [Ni(dmit)$_2$]$^{-}$ (1)

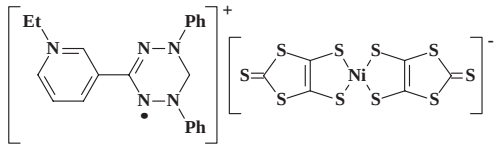

[*m*-EtPyDV]$^{+}$[Ni(dmit)$_2$]$^{-}$ (2)

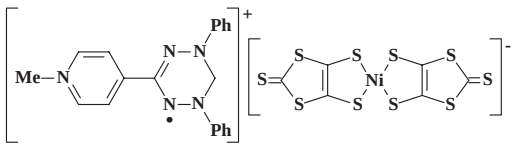

[*p*-MePyDV]$^{+}$[Ni(dmit)$_2$]$^{-}$ (3)

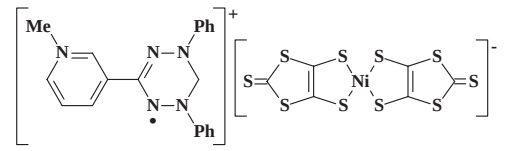

[*m*-MePyDV]$^{+}$[Ni(dmit)$_2$]$^{-}$ (4)

Fig. 1. Chemical structures of the 1:1 salts of 3-(4- and 3-alkyl-pyridinium)-1,5-diphenylverdazyl radical cations (alkyl = ethyl and methyl) with Ni(dmit)$_2$ anion.

charge-transfer salts **1**–**4** are as follows.

[*p*-EtPyDV]$^{+}$[Ni(dmit)$_2$]$^{-}$ (1): To a stirred solution of [*p*-EtPyDV]$^{+}$I^{-} (47.0 mg, 0.100 mmol) in methanol (50 mL), [*n*-Bu$_4$N]$^{+}$[Ni(dmit)$_2$]$^{-}$ (69.4 mg, 0.100 mmol) in methanol (250 mL) was added, followed by stirring for 2 h under a nitrogen atmosphere. The black-violet solids precipitated were filtered and washed with diethyl ether. Recrystallization of the residue from acetonitrile–diethyl ether afforded the product as black-violet prismatic crystals (43 mg, 54%): mp 190.0–191.5 °C; UV (acetonitrile) λ_{max} (log ε) 747 (3.37), 617 (3.59), 543 (4.03), 436 (4.26), 380 (4.56), 315 (4.59), 241 (4.64). Found: C, 40.58; H, 2.62; N, 8.46%. Calcd for $C_{27}H_{21}N_5S_{10}Ni$: C, 40.80; H, 2.66; N, 8.81%. The radical salts **2**, **3**, and **4** were prepared similarly.

[*m*-EtPyDV]$^{+}$[Ni(dmit)$_2$]$^{-}$ (2): Dark-green powder crystals: mp 199.0–201.0 °C; UV (acetonitrile) λ_{max} (log ε) 735 (3.59), 625 (3.64), 443 (4.31), 389 (4.39), 314 (4.64), 240 (4.58). Found: C, 40.67; H, 2.61; N, 8.71%. Calcd for $C_{27}H_{21}N_5S_{10}Ni$: C, 40.80; H, 2.66; N, 8.81%.

[*p*-MePyDV]$^{+}$[Ni(dmit)$_2$]$^{-}$ (3): Dark-green powder crystals: mp > 300.0 °C; UV (acetonitrile) λ_{max} (log ε) 747 (3.36), 619 (3.59), 543 (4.13), 436 (4.26), 379 (4.56), 350 (4.51), 315 (4.60), 240 (4.65). Found: C, 40.82; H, 2.57; N, 9.14%. Calcd for $C_{26}H_{19}N_5S_{10}Ni$: C, 39.99; H, 2.45; N, 8.97%.

[*m*-MePyDV]$^{+}$[Ni(dmit)$_2$]$^{-}$ (4): Black-violet powder crystals: mp > 300.0 °C; UV (acetonitrile) λ_{max} (log ε) 736 (3.34), 619 (3.61), 439 (4.30), 392 (4.41), 315 (4.58), 241 (4.63). Found: C, 40.15; H, 2.55; N, 9.05%. Calcd for $C_{26}H_{19}N_5S_{10}Ni$: C, 39.99; H, 2.45; N, 8.97%.

Measurements. The magnetic susceptibility (χ_M) was measured in the temperature range of 1.8–300 K by a SQUID magnetometer. The χ_M of all of the samples has been corrected for the diamagnetic contribution ($\chi_{dia} = -0.399 \times 10^{-3}$ emu/mol for salts **1** and **2** and -0.388×10^{-3} emu/mol for salts **3** and **4**), calculated by Pascal's method. The conductivity measurements of salts **1**–**4** were performed for pressed pellet samples of the salts, using the standard dc four-probe method.

Structure Determination. The X-ray measurements of the [*p*-EtPyDV]$^{+}$[Ni(dmit)$_2$] salt (**1**) and [*p*-EtPyDV]$^{+}$I^{-} salt (**5**) were carried out on a Rigaku AFC5R diffractometer with graphite-monochromated Mo Kα ($\lambda = 0.71069$ Å) radiations. The structure was solved by the direct method.

Crystallographic data for the structural analysis have been deposited with the Cambridge Crystallographic Data Centre, deposition numbers CCDC-249719 and -249720. Copies of this information may be obtained free of charge from: The Director, CCDC, 12 Union Road, Cambridge, CB2 1EZ, UK (Fax: +44 1223 336033; e-mail: deposit@ccdc.cam.ac.uk or www: http://www.ccdc.cam.ac.uk/conts/retrieving.html).

Results

UV and Visible Spectra of Salts 1–4. The absorption spectra of salts **1**–**4** in acetonitrile can be well explained by an addition of those of iodide salts **5**–**8** and [*n*-Bu$_4$N]$^{+}$-[Ni(dmit)$_2$]$^{-}$, respectively. The result suggests the 1:1 complex formation between the verdazyl cation and Ni(dmit)$_2$ anion.[22] The electronic structures of the verdazyl radical cation and Ni(dmit)$_2$ anion moieties in salts **1**–**4** are thought to be similar to those corresponding in iodide salts **5**–**8** and [*n*-Bu$_4$N]$^{+}$-[Ni(dmit)$_2$]$^{-}$, respectively.

Crystal Structures of Salts 1 and 5. The crystal structure was determined for the [*p*-EtPyDV]$^{+}$[Ni(dmit)$_2$]$^{-}$ salt (**1**) and the [*p*-EtPyDV]$^{+}$I^{-} salt (**5**) (see Table 1). In Figs. 2a and b, we show the molecular structures of salts **1** and **5**, respectively. Table 2 shows that the bond lengths and bond angles of verdazyl moieties (N1–N2–C1–N3–N4–C2) in salts **1** and **5** are similar to those corresponding in neutral 1,3,5-triphenylverdazyl (TPV),[32] indicating that the verdazyl moieties in salts **1** and **5** are not oxidized.[33] However, the dihedral angles (8.965 and 2.380°) between the least-squares plane (N1–N2–N3–N4 plane) of the verdazyl ring and those of N1- and N4-phenyl rings in salt **1** are much smaller than those of the iodide salt **5** (9.255 and 28.925°) and TPV (27.8(4) and 40.2(4)°), respectively. In TPV, the verdazyl ring has an unsymmetrical boat configuration, with both C1 and C2 out of the nitrogen plane on the same side. C1 is displaced by only +0.099 Å, while C2 is displaced by +0.590 Å. The verdazyl ring in the iodide salt **5** also shows a similar structure to that of TPV. On the other hand, in salt **1**, the verdazyl ring has an unsymmetrical chair configuration, although the deviations (−0.007(16) and +0.140(17) Å) of the C1 and C2 atoms out of the N1–N2–N3–N4 plane are very small, indicating that the verdazyl molecule has a planar structure. The iodide ion (I^{-}) in salt **5** is located at a position near the C12, C16, C8, and C18 atoms of the phenyl rings; the I–C12, I–C16, I–C8, and I–C18 distances are 3.720(4), 3.929(4), 3.942(4), and 3.960(5) Å, respectively. On the other hand, the distances between the I^{-} ions and the neighboring nitrogen atoms (N5) having positive charge are I–N5 = 4.204(4), 4.461(4), and 4.522(4) Å.

Table 1. Crystal Data, Experimental Conditions, and Refinement Details of Salts **1** and **5**

	[*p*-EtPyDV]$^+$[Ni(dmit)$_2$]$^-$ (**1**)	[*p*-EtPyDV]$^+$I$^-$ (**5**)
Empirical formula	$C_{27}H_{21}N_5NiS_{10}$	$C_{21}H_{21}N_5I$
Formula weight	794.80	470.33
Crystal color	Black, prismatic	Purple, prismatic
Crystal system	triclinic	monoclinic
Space group	$P\bar{1}$ (#2)	$P2_1/c$ (#14)
a/Å	11.866(3)	8.771(2)
b/Å	16.556(4)	8.851(3)
c/Å	9.267(2)	26.166(2)
α/°	105.94(2)	
β/°	111.93(2)	96.83(1)
γ/°	79.72(3)	
V/Å^3	1618.0(8)	2016.8(8)
Z	2	4
D_x/g cm^{-3}	1.631	1.549
μ/cm^{-1}	12.74 (Mo Kα)	16.04 (Mo Kα)
Crystal size/mm^3	0.03 × 0.10 × 0.50	0.25 × 0.23 × 0.10
No. of reflections measured	5999	5262
No. of unique reflections (R_{int})	5745 (0.079)	4641 (0.026)
R, R_w	0.180, 0.221	0.067, 0.101

Table 2. Selected Structural Data of 1,3,5-Triphenylverdazyl (TPV), [*p*-EtPyDV]$^+$I$^-$ Salt (**5**), and [*p*-EtPyDV]$^+$[Ni(dmit)$_2$]$^-$ Salt (**1**)

	TPV	[*p*-EtPyDV]$^+$I$^-$ (**5**)	[*p*-EtPyDV]$^+$[Ni(dmit)$_2$]$^-$ (**1**)
N1–N2/Å[a]	1.351(3)	1.350(5)	1.34(2)
N2–C1/Å[b]	1.338(1)	1.335(6)	1.33(1)
N1–C2/Å[c]	1.443(3)	1.452(6)	1.43(2)
N1–N2–C1/deg[d]	114.4(2)	114.3(4)	115.4(9)
N2–C1–N3/deg	126.8	128.3(4)	128(1)
N3–N4–C2/deg[e]	117.8(4)	117.9(4)	123.7(9)
N1–C2–N4/deg	106.1	107.4(4)	112(1)
C1/Å[f]	+0.099	+0.078(6)	−0.007(16)
C2/Å[f]	+0.590	+0.561(7)	+0.140(17)
Dihedral angle/deg N1–C3–(Phenyl)	27.8(4)	9.255	8.965
Dihedral angle/deg N4–C15–(Phenyl)	40.2(4)	28.925	2.380
Dihedral angle/deg C1–C9–(Phenyl)	7.0(5)	3.757	7.148

a) Mean value of N1–N2 and N3–N4. b) Mean value of N2–C1 and N3–C1. c) Mean value of N1–C2 and N4–C2. d) Mean value of N1–N2–C1 and N4–N3–C1. e) Mean value of N3–N4–C2 and N2–N1–C2. f) Deviation out of the N1–N2–N3–N4 plane.

The bond lengths and bond angles of the Ni(dmit)$_2$ anion in salt **1** are also similar to those corresponding in the [*n*-Bu$_4$N]$^+$-[Ni(dmit)$_2$]$^-$ salt (data are not shown).[34] The result indicates that the Ni(dmit)$_2$ moiety in salt **1** is considered to exist as a mono anion [Ni(dmit)$_2$]$^-$ with $S = 1/2$.[6] The dihedral angle between the least-squares planes of the two dmit rings in salt **1** is 4.683°, indicating the planarity of the Ni(dmit)$_2$ moiety.

Molecular packing of salt **1** is shown in Fig. 3a. The unit cell of salt **1** contains two Ni(dmit)$_2$ anions and two verdazyl cations [*p*-EtPyDV]$^+$. The Ni(dmit)$_2$ anion molecules in salt **1** form a dimer ([Ni(dmit)$_2$]$^-$ (A)–[Ni(dmit)$_2$]$^-$ (B)) having intra-dimer contacts of ca. 3.6–3.8 Å (see Table 3). The dimer molecules are sandwiched between two verdazyl cation molecules, forming a linear tetramer ([*p*-EtPyDV]$^+$ (A)–[Ni(dmit)$_2$]$^-$ (A)–[Ni(dmit)$_2$]$^-$ (B)–[*p*-EtPyDV]$^+$ (B)) in the crystal. The Ni(dmit)$_2$ anion dimers are connected to each other through short S–S contacts (S8–S9 = 3.566(4) Å, S9–S9 = 3.811(7) Å, and S5–S8 = 3.934(5) Å) between Ni(A) and Ni(C).

Conductivities of Salts 1–4. The room-temperature conductivities (σ_{RT}'s) for salts **1**, **2**, **3**, and **4** are 2.3×10^{-5}, 1.8×10^{-4}, 1.4×10^{-5}, and 5.4×10^{-6} S cm^{-1}, respectively, as listed in Table 4. The temperature dependency of the resistivities of salts **1**–**4** are shown in Fig. 4. Under ambient pressure, salts **1**–**4** show semiconductive behavior with activation energy values (E_A's) of 0.28, 0.52, 0.21, and 0.33 eV at the temperature range of 219–298, 250–283, 246–279, and 269–298 K, respectively.

Magnetic Susceptibilities of Salts 1–4. Figure 5 shows a plot of $\chi_M T$ versus T for salts **1**–**4**. The value of $\chi_M T$ for the

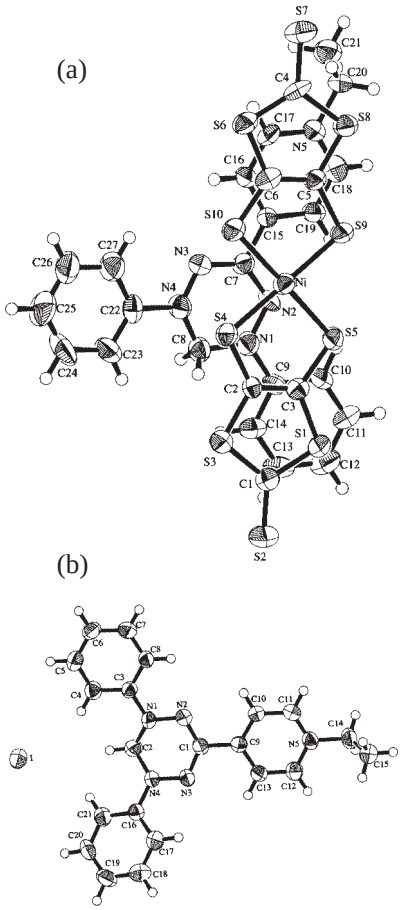

Fig. 2. Molecular structures of (a) the $Ni(dmit)_2$ salt (**1**) and (b) the iodide salt (**5**) with the atom numbering scheme.

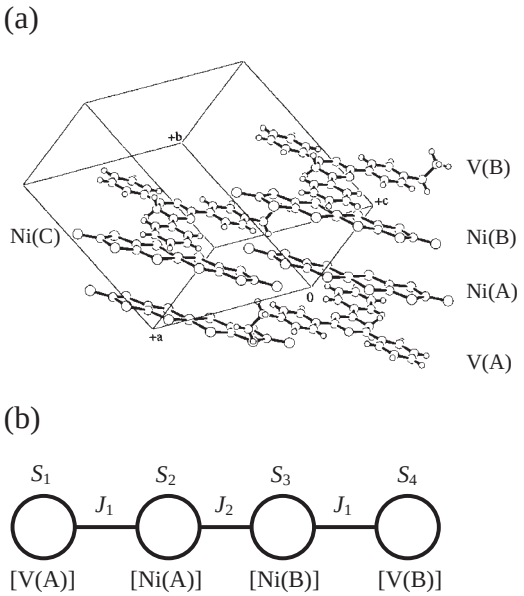

Fig. 3. (a) Molecular packing in salt **1**, showing the formation of magnetic linear tetramer, [verdazyl cation (A)–$Ni(dmit)_2$ anion (A)–$Ni(dmit)_2$ anion (B)–verdazyl cation (B)]. (b) Scheme 1.

$[p\text{-EtPyDV}]^+[Ni(dmit)_2]^-$ salt (**1**) is 0.243 K emu mol^{-1} at 300 K (see Table 4), and decreases by lowering the temperature, indicating AFM interactions in salt **1**. As shown in Fig. 6, the χ_M of salt **1** decreases slowly by lowering the temperature from 300 K with a minimum at around 160 K, and increases rapidly below 20 K.

The value of $\chi_M T$ for the $[m\text{-EtPyDV}]^+[Ni(dmit)_2]^-$ salt (**2**) is 0.685 K emu mol^{-1} at 300 K, and is close to the sum of those (0.376 and 0.392 K emu mol^{-1}) expected for non-interacting $S = 1/2$ spin system with g-values ($g_V{}^+ = 2.0032$ for $[m\text{-EtPyDV}]^+I^-$ (**6**) and $g_{Ni}{}^- = 2.0472$ for $[n\text{-Bu}_4N]^+[Ni(dmit)_2]^-$ (see Table 5)), respectively, suggesting that both the spins of the verdazyl cation and the $Ni(dmit)_2$ anion contribute to the magnetism of salt **2**. $\chi_M T$ for salt **2** decreases gradually by decreasing the temperature with a plateau between 60 and 30 K, followed by an increase with decreasing temperature. Below 30 K, the susceptibility of salt **2** follows the Curie–Weiss law with a Curie constant of 0.376 K emu mol^{-1} and a positive Weiss constant of $+2.2 \pm 0.2$ K (see Fig. 7b). The $\chi_M T$ (0.388 K emu mol^{-1}) of salt **2** at the plateau (30–60 K) amounts to about one half of the value (0.768 K emu mol^{-1}) calculated on the basis of two $S = 1/2$ spins per one formula unit of the salt, as shown in Fig. 7a. The additional susceptibility above 60 K is considered to be a thermally activated species which is nonmagnetic at lower temperatures. This magnetic contribution is tentatively assigned to the dimer of the $Ni(dmit)_2{}^-$ radical anions.[22,23] The susceptibility at lower temperatures is, therefore, attributed to the verdazyl radical cations.

Table 3. Pertinent Intermolecular Contacts (r/Å) in $[p\text{-EtPyDV}]^+[Ni(dmit)_2]^-$ (**1**)

Ni (A)–Ni (B)	Ni (A)–Ni (C)	Ni (A)–V (A)	V (A)–V (B)
Ni–Ni 4.278(3)	Ni–Ni > 5.00		N(i)–N(j) (i, j = 1, 2, 3, and 4)
(r < 4.00 Å)	(r < 4.00 Å)	(r < 4.00 Å)	(r < 5.00 Å)
Ni–S10 3.815(4)	S5–S8 3.934(5)	Ni–N2 3.771(9)	N1–N1 4.29(2)
Ni–C6 3.87(1)	S8–S9 3.566(4)	Ni–N3 3.684(9)	
S2–S7 3.970(5)	S9–S9 3.811(7)	S4–N1 3.936(9)	
S3–S7 3.614(5)		S4–N3 3.69(1)	
S4–S8 3.819(5)		S4–N4 3.30(1)	
S4–C5 3.59(1)		S5–N1 3.79(1)	
S4–C6 3.81(1)		S5–N2 3.67(1)	
C2–C4 3.63(2)		S10–N3 3.597(9)	
		C2–N1 3.62(2)	
		C2–N4 3.90(1)	
		C3–N1 3.56(1)	

Table 4. Conductivity (σ_{RT}), Activation Energy (E_A), $\chi_M T$ Value (at 300 K), and Magnetism of Salts **1–4**

Salts	σ_{RT} /S cm^{-1}	E_A /eV	$\chi_M T$ /K emu mol^{-1}	Magnetism
[*p*-EtPyDV]$^+$ [Ni(dmit)$_2$]$^-$ (**1**)	2.3×10^{-5} (at 298 K)	0.28	0.243	Linear tetramer ($2J_1/k_B = -780$ K, $2J_2/k_B = -200$ K) + Curie impurity (5.3%)
[*m*-EtPyDV]$^+$ [Ni(dmit)$_2$]$^-$ (**2**)	1.8×10^{-4} (at 283 K)	0.52	0.685	1D-Ferro ($2J/k_B = +2.5$ K) + S–T ($2J/k_B = -320$ K)
[*p*-MePyDV]$^+$ [Ni(dmit)$_2$]$^-$ (**3**)	1.4×10^{-5} (at 279 K)	0.21	0.288	Linear tetramer
[*m*-MePyDV]$^+$ [Ni(dmit)$_2$]$^-$ (**4**)	5.4×10^{-6} (at 298 K)	0.33	0.713	Alternating Chain ($T_{max} = 100 \pm 2$ K, $2J_1/k_B = -165$ K, $\alpha = J_2/J_1 = 0.6$) + Curie impurity (5.4%)

Table 5. The *g*-Value and Peak-to-Peak Line-Width (ΔH_{PP}) of Salts **1–8** and [(*n*-Bu)$_4$N]$^+$[Ni(dmit)$_2$]$^-$

Salts	300 K		77 K	
	g-Value	ΔH_{PP}/mT	*g*-Value	ΔH_{PP}/mT
[*p*-EtPyDV]$^+$[Ni(dmit)$_2$]$^-$ (**1**)	2.0221[a]	28.4	2.0231[c]	8.75
[*m*-EtPyDV]$^+$[Ni(dmit)$_2$]$^-$ (**2**)	2.0093[a]	31.3	2.0070[d]	14.0
[*p*-MePyDV]$^+$[Ni(dmit)$_2$]$^-$ (**3**)	2.0213[a]	27.1	2.0241[d]	14.31
[*m*-MePyDV]$^+$[Ni(dmit)$_2$]$^-$ (**4**)	2.0206[a]	9.56	2.0194[c]	8.60
[*p*-EtPyDV]$^+$I$^-$ (**5**)	2.0039[b]	0.414	2.0037	0.346
[*m*-EtPyDV]$^+$I$^-$ (**6**)	2.0032[b]	0.340	2.0032	0.324
[*p*-MePyDV]$^+$I$^-$ (**7**)	2.0037[b]	0.444	2.0037	0.373
[*m*-MePyDV]$^+$I$^-$ (**8**)	2.0033[b]	0.351	2.0034	0.379
[(*n*-Bu)$_4$N]$^+$[Ni(dmit)$_2$]$^-$	2.0472[a]	7.97	2.0474	7.94

a) Experimental error: ±0.0005. b) Experimental error: ±0.0001. c) The value at 103 K. At the temperature below 103 K, the signal due to Curie impurity overlaps to that of salt **1**, and the *g*-value and linewidth could not be determined. d) The value at 173 K.

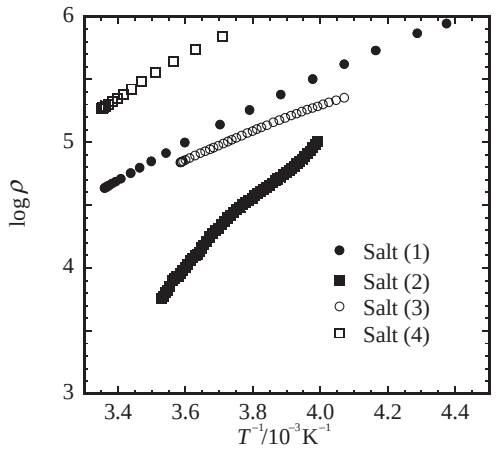

Fig. 4. Temperature dependence of the resistivity (ρ) of the 1:1 salts **1–4** at ambient pressure.

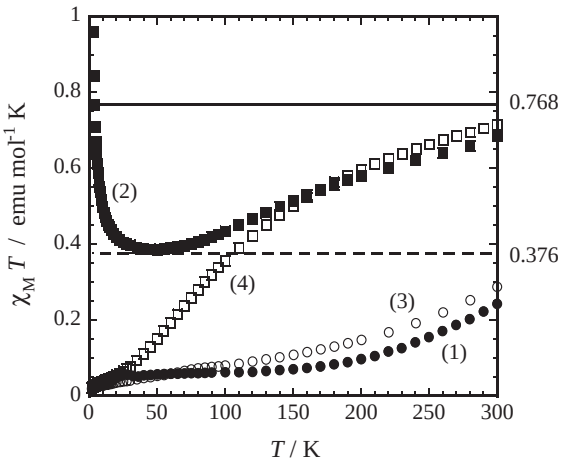

Fig. 5. Temperature dependence of the product $\chi_M T$ for salts **1–4**.

The χ_M of the [*p*-MePyDV]$^+$[Ni(dmit)$_2$]$^-$ salt (**3**) decreases gradually by decreasing temperature from 300 K with a minimum at about $T_{min} = 170$ K (data are not shown). The susceptibility increases below 170 K by decreasing temperature. The value of $\chi_M T$ for **3** is 0.288 K emu mol^{-1} at 300 K, and decreases by lowering the temperature, indicating AFM interactions in **3**, as shown in Fig. 5. The magnetic behavior of salt **3** is very similar to that of salt **1**.

The χ_M of the [*m*-MePyDV]$^+$[Ni(dmit)$_2$]$^-$ salt (**4**) shows a broad maximum at $T_{max} = 100 \pm 2$ K, as shown in Fig. 8. An increase in susceptibility below 26 K was observed, which is probably due to Curie impurities. The value (0.713 K emu mol^{-1}) of $\chi_M T$ at 300 K observed for salt **4** is similar to the sum of those (0.376 and 0.392 K emu mol^{-1}) for a $S = 1/2$ spin system with $g_V{}^+ = 2.0033$ and $g_{Ni}{}^- = 2.0472$ (see Table 5), suggesting that both the spins of the verdazyl cation and Ni(dmit)$_2$ anion contribute to the magnetism of salt **4**.

ESR Measurements of Salts 1–8. The ESR measurements

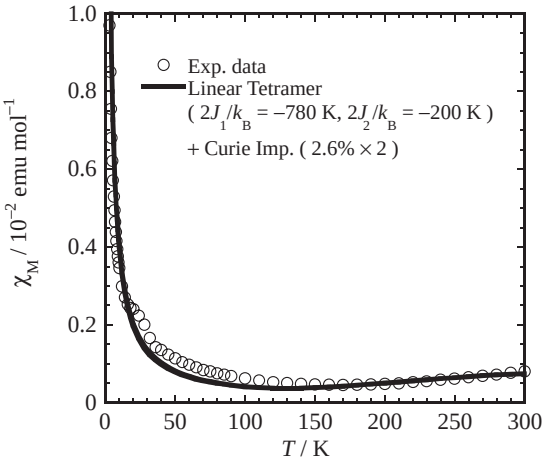

Fig. 6. Temperature dependence of the magnetic susceptibility of salt **1**. The solid curve is the theoretical susceptibility calculated using Eq. 2 in Ref. 35.

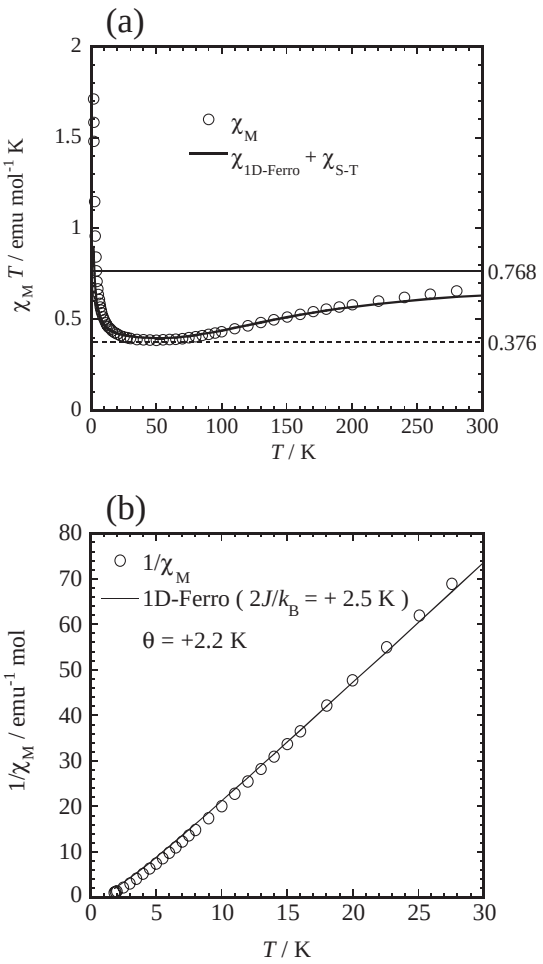

Fig. 7. (a) Temperature dependence of the product $\chi_M T$ (○) for salt **2**. The solid curve is the theoretical susceptibility calculated using Eq. 2. (b) Inverse molar magnetic susceptibility ($1/\chi_M$) of salt **2** at low temperatures. The observed values (○) obey the theoretical results for the 1D isotropic Heisenberg ferromagnet (Eq. 3) with $2J/k_B = +2.5$ K indicated by the solid line.

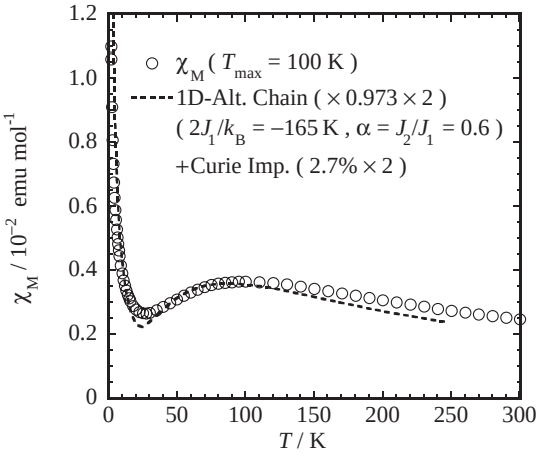

Fig. 8. Temperature dependence of the magnetic susceptibility (χ_M) (○) of salt **4**. The dashed curve is the theoretical susceptibility calculated by using Eq. 5.

were carried out in powder samples of salts **1**–**8** and [*n*-Bu_4N]$^+$[Ni(dmit)$_2$]$^-$ in the temperature range of 77–300 K. The *g*-value and the peak-to-peak line-width (ΔH_{PP}) of the samples at 300 and 77 K are listed in Table 5. The ESR spectra of the iodide salts **5**–**8** show an exchange-narrowed, Lorentz-type absorption located at $g_V{}^+ = 2.0032$–2.0039 with line-widths (ΔH_{PP}) of 0.340–0.444 mT. Both the *g*-values and the line-widths are nearly temperature independent (see Figs. 9 and 10), as observed for usual organic radical solids. The ESR spectrum of the [*n*-Bu_4N]$^+$[Ni(dmit)$_2$]$^-$ salt exhibits one symmetric broad line with a $g_{Ni}{}^-$-value of 2.0472 and a line-width of 7.97 mT at 300 K. Both the *g*-value and the line-width are temperature-independent (see Fig. 9). A relatively large *g*-value and line-width are characteristics of the Ni(dmit)$_2$ radical anion.[6]

The ESR spectra of salts **1**–**4** also exhibit one symmetric broad line with a line-width of 28.4, 28.8, 27.1, and 9.56 mT at 300 K, respectively. The temperature dependencies of the *g*-value and line-width of salts **1**–**4** are shown in Figs. 9 and 10.

Discussion

Magnetic Properties of Salts 1 and 3. The χ_M of salt **1** is shown in Fig. 6. As described in a previous section, the Ni(dmit)$_2$ anion molecules in salt **1** form a dimer ([Ni(dmit)$_2$]$^-$ (A)–[Ni(dmit)$_2$]$^-$ (B)) with short intra-dimer contacts of ca. 3.6–3.7 Å, suggesting strong AFM exchange interactions. However, the χ_M of **1** can not be explained by a dimer model. In salt **1**, the dimer molecules are sandwiched between two verdazyl cation [*p*-EtPyDV]$^+$ molecules, forming a linear tetramer ([*p*-EtPyDV]$^+$ (A)–[Ni(dmit)$_2$]$^-$ (A)–[Ni(dmit)$_2$]$^-$ (B)–[*p*-EtPyDV]$^+$ (B)) (see Fig. 3 and Table 3). As described in a previous section, the verdazyl cation molecule in salt **1** has a planar structure, and we can expect close contacts between the verdazyl cation and Ni(dmit)$_2$ anion molecules. In fact, there are many short contacts between the Ni, S(*i*), and C(*i*) atoms in the Ni(dmit)$_2$ anions and the N(*j*) atoms ($j = 1$, 2, 3, and 4) in the hydrazidinyl moiety (N1–N2–C7–N3–N4–C8), which have large unpaired spin densities, of verdazyl cations.[20] The result suggests strong exchange interactions between the

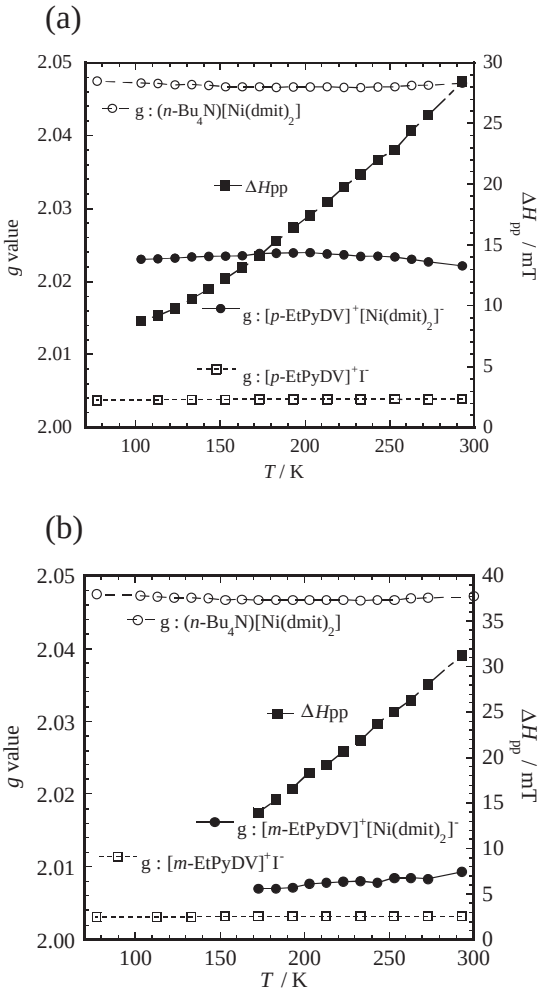

Fig. 9. Temperature dependence of the g-value ($g(T)$) (●) and the line-width ($\Delta H_{PP}(T)$) (■) of the polycrystalline sample of (a) salt **1** and (b) salt **2**.

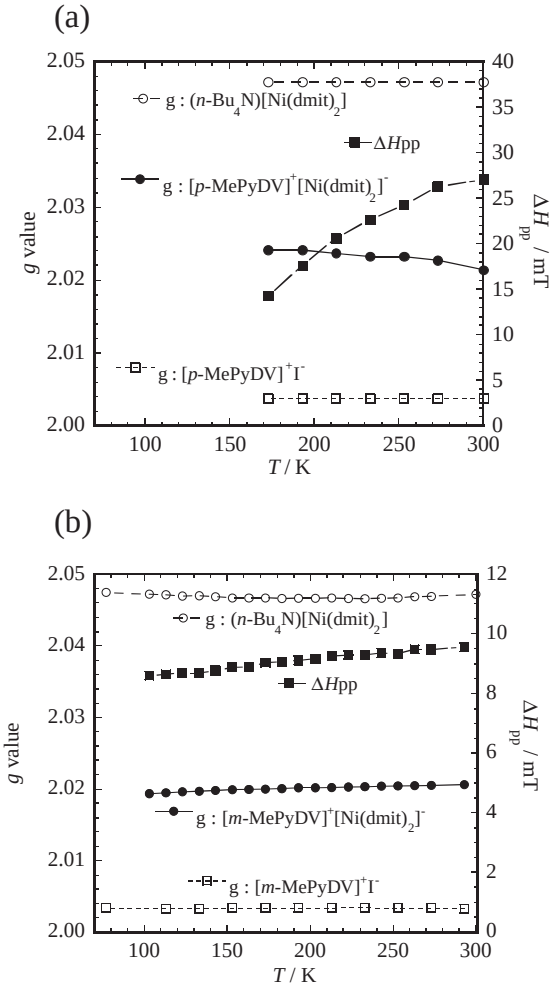

Fig. 10. Temperature dependence of the g-value ($g(T)$) (●) and the line-width ($\Delta H_{PP}(T)$) (■) of the polycrystalline sample of (a) salt **3** and (b) salt **4**.

verdazyl cation and the Ni(dmit)$_2$ anion molecules.

When the exchange energy ($2J/k_B$) between verdazyl cation spin ($S = 1/2$) and Ni(dmit)$_2$ anion spin ($S = 1/2$) is large compared to the g-value difference ($\Delta g = |g_V{}^+ - g_{Ni}{}^-|$) of the parent verdazyl radical cation and Ni(dmit)$_2$ anion, the ESR spectrum from a solid of salt **1** is centered at a position between the absorption lines from the parent species.[35] In fact, the g-value (2.0221) of **1** at 300 K is similar to the average value ($g_{AV} = 2.0256$) of the verdazyl radical cation ($g_V{}^+ = 2.0039$) and Ni(dmit)$_2$ anion ($g_{Ni}{}^- = 2.0472$). The g-value of salt **1** remains constant when lowering the temperature, as shown in Fig. 9a.

In such a case, the χ_M of salt **1** may be explained by a four-spin Heisenberg Hamiltonian,

$$H = -2J_1(S_1S_2 + S_3S_4) - 2J_2S_2S_3 \quad (1)$$
$$S_1 = S_2 = S_3 = S_4 = 1/2,$$

where J_1 is the exchange interaction between an edge verdazyl cation and a central Ni(dmit)$_2$ anion and J_2 is the interaction between two central Ni(dmit)$_2$ anions. The model is shown in Fig. 3b. This Hamiltonian has been solved exactly by Rubenacker et al.[36] to obtain the energy levels and magnetic susceptibility. Using Eq. 2 in Ref. 36, we have fitted our data to this model, where the g-value observed for **1** was used tentatively for the calculation of the susceptibility. The calculated susceptibility is shown by a solid curve in Fig. 6. The best fit parameters obtained are $2J_1/k_B = -780$ K and $2J_2/k_B = -200$ K. The $2J_2/k_B$ value (−200 K) for the dimer is similar to that (−320 K) for the Ni(dmit)$_2$ dimer in salt **2**, as described later.

Recently, two examples of a magnetic linear tetramer with (i) $2J_1/k_B = -600$ K and $2J_2/k_B = -280$ K and (ii) $2J_1/k_B = -30$ K and $2J_2/k_B = -580$ K have also been reported for the salts of 6-oxo-verdazyl radical cations with the Ni(dmit)$_2$ anion.[23] Additionally, the formations of the Ni(dmit)$_2$ dimer have been reported for three kinds of salts of 6-oxo-verdazyl radical cations with the Ni(dmit)$_2$ anion, giving the $2J_2/k_B$ values of −258, −274, and −354 K.[22,23] The $2J_1/k_B$ and $2J_2/k_B$ values reported are similar to those ($2J_1/k_B = -780$ K and $2J_2/k_B = -200$ K) obtained for salt **1**.

The Ni(dmit)$_2$ (A) molecule connects with the Ni(dmit)$_2$ (C) molecule with short inter-dimer S···S contacts (see Fig. 3a and Table 3). Therefore, we can expect some interaction between the two Ni(dmit)$_2$ molecules (A) and (C), that is, between

neighboring linear tetramers ([*p*-EtPyDV]$^+$ (A)–[Ni(dmit)$_2$]$^-$ (A)–[Ni(dmit)$_2$]$^-$ (B)–[*p*-EtPyDV]$^+$ (B)). The difference between the experimental and theoretical values of susceptibility of salt **1** may be due to such an interaction. However, the details are not clear at present.

The susceptibility of the [*p*-MePyDV]$^+$[Ni(dmit)$_2$]$^-$ salt (**3**) is similar to that of salt **1**. The temperature dependencies of the *g*-value and line-width of salt **3** are also similar to those of salt **1**, as shown in Fig. 10a. The result suggests that salt **3** forms a magnetic linear tetramer as observed for salt **1**, although the crystal structure of salt **3** has not been determined.

Magnetic Property of Salt 2. The susceptibility of salt **2** can be explained by two term contributions (Eq. 2).

$$\chi_{\mathrm{M}} = \chi_{\text{1D-Ferro}} + \chi_{\text{S–T}}, \tag{2}$$

where the first and second terms represent the contributions from the quasi-one-dimensional (1D) FM Heisenberg linear-chain system[37] and singlet–triplet (S–T) equilibrium system, respectively. $\chi_{\text{1D-Ferro}}$ and $\chi_{\text{S–T}}$ are given by Eqs. 3 and 4, respectively.

$$\chi_{\text{1D-Ferro}} = (N_{\mathrm{o}} g^2 \mu_{\mathrm{B}}{}^2 / 4k_{\mathrm{B}}T)[1 + (J/k_{\mathrm{B}}T)], \tag{3}$$

$$\chi_{\text{S–T}} = (N_{\mathrm{o}} g^2 \mu_{\mathrm{B}}{}^2 / k_{\mathrm{B}}T)[1/(3 + \mathrm{e}^{-2J/k_{\mathrm{B}}T})]. \tag{4}$$

The susceptibility of salt **2** follows the Curie–Weiss law with a positive Weiss constant of +2.2 K in the temperature region between 10 and 40 K. A plot of $1/\chi_{\mathrm{M}}$ against T is no longer linear at low temperature (<10 K). Therefore, the low-temperature behavior of the susceptibility of salt **2** was analyzed on the basis of the quasi-1D FM Heisenberg model. In fact, the susceptibilities of salt **2** below 40 K are well reproduced by Eq. 3 with $2J/k_{\mathrm{B}} = +2.5 \pm 1.0$ K and $g = 2.00$ as shown in Fig. 7b. Above ca. 50 K, $\chi_{\mathrm{M}}T$ increases with increasing temperature, as shown in Fig. 7a. This increase indicates that thermal magnetic excitation occurs in addition to the 1D FM linear-chain spins. The experimental data were interpreted by the S–T model (Eq. 4) with $2J/k_{\mathrm{B}} = -320$ K. As shown in Fig. 7a, the experimental curve can be well reproduced by Eq. 2. The value of the exchange interaction ($2J/k_{\mathrm{B}} = -320$ K) for salt **2** is similar to those of $2J_2/k_{\mathrm{B}}$ (−258–−580 K) observed for the Ni(dmit)$_2$ anion dimers in the salts between 6-oxo-verdazyl radical cations and the Ni(dmit)$_2$ anion, as described above.[22,23] Consequently, $\chi_{\text{1D-Ferro}}$ and $\chi_{\text{S–T}}$ in Eq. 2 for salt **2** are due to the verdazyl radical cation and Ni(dmit)$_2$ anion dimer, respectively.

If the verdazyl cation and Ni(dmit)$_2$ anion spins form two magnetically-independent subsystems in the crystal, the *g*-value will decrease from the average value ($g_{\mathrm{AV}} = 2.0252$) of the verdazyl radical cation ($g_{\mathrm{V}}{}^+ = 2.0032$) and Ni(dmit)$_2$ anion ($g_{\mathrm{Ni}}{}^- = 2.0472$) at 300 K to that of the verdazyl radical cation ($g_{\mathrm{V}}{}^+ = 2.0032$) at 77 K.[22,23,38] In fact, the *g*-value (2.0070) of salt **2** observed at 173 K is similar to that (2.0032) of the iodide salt **6**. However, the *g*-value (2.0093) of salt **2** observed at 300 K is much smaller than that expected, as shown in Fig. 9b. The reason is not clear at present.

Magnetic Property of Salt 4. The susceptibility of the [*m*-MePyDV]$^+$[Ni(dmit)$_2$]$^-$ salt (**4**) shows a broad maximum at $T_{\mathrm{max}} = 100 \pm 2$ K. The susceptibility of **4** can be well explained by the sum of two contributions:

$$\chi_{\mathrm{M}} = C_{\text{1D-Alt}}\chi_{\text{1D-Alt}} + C_{\text{Curie}}\chi_{\text{Curie}}, \tag{5}$$

where $C_{\text{1D-Alt}} + C_{\text{Curie}} = 2$, and the first and second terms represent the contributions from the 1D AFM Heisenberg alternating-chain system[39] and from the Curie impurity, respectively. C_{i} is the fraction of each term. The dashed curve in Fig. 8 is a theoretical curve with $C_{\text{1D-Alt}} = 2 \times 0.973$ and $C_{\text{Curie}} = 2 \times 0.027$ and $2J_1/k_{\mathrm{B}} = -165$ K (alternation parameter $\alpha = J_2/J_1 = 0.6$). The result shows that both the spins of the verdazyl cation and Ni(dmit)$_2$ anion contribute to the magnetism of salt **4**.

As shown in Fig. 10b, the *g*-value (2.0206 at 300 K) of salt **4** is almost temperature-independent, and is similar to the average value ($g_{\mathrm{AV}} = 2.0252$) of the verdazyl radical cation ($g_{\mathrm{V}}{}^+ = 2.0033$) and Ni(dmit)$_2$ anion ($g_{\mathrm{Ni}}{}^- = 2.0472$), suggesting that the verdazyl cation and Ni(dmit)$_2$ anion molecules form a 1D alternating-chain in the crystal.[35] The result shows to be in good accordance with that obtained by susceptibility measurements.

Conducting Properties of Salts 1–4. Recently, we prepared several kinds of 1:1 and 1:3 salts of open-shell 6-oxo-verdazyl radical cations with the Ni(dmit)$_2$ anion, and found that the 1:3 salts are molecular paramagnetic semiconductors.[22,23] On the other hand, the 1:1 salts showed properties of paramagnetic insulators, as observed for the usual 1:1 salts of the Ni(dmit)$_2$ anion with closed-shell electron donor cations, such as tetraalkylammonium cations, alkali metal cations, etc.[1–5] However, in the present work, the 1:1 salts **1**–**4** studied were found to be semiconductors, against to our expectation.

Generally, organic free radical solids display properties of insulators. The semiconductive behavior of salts are due to the existence of the Ni(dmit)$_2$ anion moiety. As described earlier, salt **1** forms a magnetic linear tetramer in which a strong exchange interaction ($2J_1/k_{\mathrm{B}} = -780$ K) was observed between Ni(dmit)$_2$ (A) anion and verdazyl (B) cation spins, in addition to that ($2J_2/k_{\mathrm{B}} = -200$ K) between Ni(dmit)$_2$ (A) and (B) anion spins. As listed in Table 3, the Ni(dmit)$_2$ anion molecules in salt **1** form a dimer with short intra-dimer contacts of ca. 3.6–3.7 Å, suggesting strong π–π interactions. In salt **1**, the dimer molecules are sandwiched between two verdazyl cation molecules, forming a magnetic linear tetramer. Actually, there are many short contacts between the atoms in the Ni(dmit)$_2$ anions and in verdazyl cations, indicating a strong π–π interaction between the verdazyl cation and the Ni(dmit)$_2$ anion molecules. Such a strong π–π interaction induces a delocalization of conduction electrons from Ni(dmit)$_2$ anion moieties to verdazyl cation moieties, and thus, a decrease in the Coulomb repulsion. Further, comparatively short S–S contacts were observed between Ni(dmit)$_2$ (A) and (C) anions (see Table 3). As a result, salt **1** may show semiconductive behavior. As salt **3** shows magnetic properties similar to those of salt **1**, we can expect strong π–π interactions in salt **3**, resulting in a decrease in the Coulomb repulsion. Further, a strong interaction between the verdazyl cation and Ni(dmit)$_2$ anion was observed for salt **4**, suggesting a decrease in the Coulomb repulsion, and thus, an increase in the conductivity in **4**. Crystal structure analyses are necessary to discuss the details of the semiconductive behavior observed for the 1:1 salts **2**–**4**.

As a conclusion, the present result shows that the 1:1 salts **1**–**4** of verdazyl cations with the $Ni(dmit)_2$ anion are new molecular magnetic semiconductors. However, the conductivities observed for these 1:1 salts are not appreciably high. It is necessary to prepare 1:2 and/or 1:3 salts to obtain magnetic conductors with high conductivity.

Summary

In the present work, four new magnetic charge-transfer salts **1**–**4** consisting of 3-(4- and 3-alkyl-pyridinium)-1,5-diphenylverdazyl (alkyl = ethyl and methyl) radical cations ($S = 1/2$) and the $Ni(dmit)_2$ anion ($S = 1/2$) ($[p\text{-EtPyDV}]^+[Ni(dmit)_2]^-$ (**1**), $[m\text{-EtPyDV}]^+[Ni(dmit)_2]^-$ (**2**), $[p\text{-MePyDV}]^+[Ni(dmit)_2]^-$ (**3**), and $[m\text{-MePyDV}]^+[Ni(dmit)_2]^-$ (**4**)) have been prepared, and their magnetic, conducting, and structural properties have been studied. Strong AFM exchange interactions between verdazyl cation and $Ni(dmit)_2$ anion molecules were observed for these salts, in addition to that between $Ni(dmit)_2$ anion molecules. The magnetic susceptibilities of salts **1** and **3** were explained by a four-spin linear tetramer model ($[Verdazyl]^+-[Ni(dmit)_2]^-[Ni(dmit)_2]^-[Verdazyl]^+$). Salts **1**–**4** are new molecular paramagnetic semiconductors. In particular, FM interactions were observed for salt **2** at 1.8–40 K. We can expect FM order for salt **2** at lower temperature. The examples of organic/inorganic hybrid systems that show magnetism and conductivity are very limited. The present work provides four examples of new molecular paramagnetic semiconductors consisting of the open-shell verdazyl radical cation and metal complex anion.

We are very grateful to Prof. Yohji Misaki and Dr. Masateru Taniguchi of Kyoto University for their help in the measurement of the conductivity of salts **2** and **3**. We are also very grateful to Prof. Katsuya Inoue and Dr. Kentaro Suzuki of the Institute for Molecular Science for their assistance in SQUID measurements. This work was partly supported by the Grant-in-Aid for Scientific Research on Priority Areas (B) of Molecular Conductors and Magnets (Area No. 730/11224205) from the Ministry of Education, Culture, Sports, Science and Technology, Japan. This work was partly supported by the Joint Study Program (2002–2003) of the Institute for Molecular Science.

References

1 L. Brossard, M. Ribault, L. Valade, and P. Cassoux, *Physica B+C (Amsterdam)*, **143**, 378 (1986).

2 A. Kobayashi, H. Kim, Y. Sasaki, K. Murata, R. Kato, and H. Kobayashi, *J. Chem. Soc., Faraday Trans.*, **86**, 361 (1990).

3 P. Cassoux, L. Valade, H. Kobayashi, A. Kobayashi, R. A. Clark, and A. E. Underhill, *Coord. Chem. Rev.*, **110**, 115 (1991).

4 A. E. Pullen and R.-M. Olk, *Coord. Chem. Rev.*, **188**, 211 (1999), and references are cited therein.

5 R. Kato, *Chem. Rev.*, **104**, 5319 (2004).

6 H. Imai, H. Otsuka, T. Naito, K. Awaga, and T. Inabe, *J. Am. Chem. Soc.*, **121**, 8098 (1999).

7 S. Aonuma, H. Casellas, C. Faulmann, B. Garreau de Bonneval, I. Malfant, P. Cassoux, P. G. Lacroix, Y. Hosokoshi, and K. Inoue, *J. Mater. Chem.*, **11**, 337 (2001).

8 R. Kuhn, F. A. Neugebauer, and H. Trischmann, *Angew. Chem.*, **67**, 691 (1964).

9 F. A. Neugebauer, H. Fisher, and C. Krieger, *J. Chem. Soc., Perkin Trans. 2*, **1993**, 535.

10 F. A. Neugebauer, H. Fisher, and R. Siegel, *Chem. Ber.*, **121**, 815 (1988).

11 K. Mukai, K. Konishi, K. Nedachi, and K. Takeda, *J. Phys. Chem.*, **100**, 9658 (1996).

12 K. Takeda, T. Hamano, T. Kawae, M. Hidaka, M. Takahashi, S. Kawasaki, and K. Mukai, *J. Phys. Soc. Jpn.*, **64**, 2343 (1995).

13 R. K. Kremer, B. Kanellakopulos, P. Bele, H. Brunner, and F. A. Neugebauer, *Chem. Phys. Lett.*, **230**, 255 (1994).

14 S. Tomiyoshi, T. Yano, N. Azuma, M. Shoga, K. Yamada, and J. Yamauchi, *Phys. Rev. B*, **49**, 16031 (1994).

15 M. Mito, H. Nakano, T. Kawae, M. Hitaka, S. Takagi, H. Deguchi, K. Suzuki, K. Mukai, and K. Takeda, *J. Phys. Soc. Jpn.*, **66**, 2147 (1997).

16 M. Mito, K. Takeda, K. Mukai, N. Azuma, M. R. Gleiter, C. Krieger, and F. A. Neugebauer, *J. Phys. Chem.*, **101**, 9517 (1997).

17 K. Mukai, N. Wada, J. B. Jamali, N. Achiwa, Y. Narumi, K. Kindo, T. Kobayashi, and K. Amaya, *Chem. Phys. Lett.*, **257**, 538 (1996).

18 K. Mukai, Y. Shimobe, J. B. Jamali, and N. Achiwa, *J. Phys. Chem. B*, **103**, 10876 (1999).

19 K. Mukai, M. Yanagimoto, S. Tanaka, M. Mito, T. Kawae, and K. Takeda, *J. Phys. Soc. Jpn.*, **72**, 2312 (2003).

20 K. Mukai, M. Matsubara, H. Hisatou, Y. Hosokoshi, K. Inoue, and N. Azuma, *J. Phys. Chem. B*, **106**, 8632 (2002).

21 K. Mukai, M. Nuwa, K. Suzuki, S. Nagaoka, N. Achiwa, and J. B. Jamali, *J. Phys. Chem. B*, **102**, 782 (1998).

22 K. Mukai, T. Hatanaka, N. Senba, T. Nakayashiki, Y. Misaki, K. Tanaka, K. Ueda, T. Sugimoto, and N. Azuma, *Inorg. Chem.*, **41**, 5066 (2002).

23 K. Mukai, N. Senba, T. Hatanaka, H. Minakuchi, K. Ohara, M. Taniguchi, Y. Misaki, Y. Hosokoshi, K. Inoue, and N. Azuma, *Inorg. Chem.*, **43**, 566 (2004).

24 K. Mukai, S. Jinno, Y. Shimobe, N. Azuma, Y. Hosokoshi, K. Inoue, M. Taniguchi, Y. Misaki, and K. Tanaka, *Polyhedron*, **20**, 1537 (2001).

25 K. Mukai, S. Jinno, Y. Shimobe, N. Azuma, M. Taniguchi, Y. Misaki, K. Tanaka, K. Inoue, and Y. Hosokoshi, *J. Mater. Chem.*, **13**, 1614 (2003).

26 M. Kurmoo, A. W. Graham, P. Day, S. J. Coles, M. B. Hursthouse, J. L. Caulfield, J. Singleton, F. L. Pratt, W. Hayes, L. Ducasse, and P. Guionneau, *J. Am. Chem. Soc.*, **117**, 12209 (1995).

27 E. Ojima, H. Fujiwara, K. Kato, H. Kobayashi, H. Tanaka, A. Kobayashi, M. Tokumoto, and P. Cassoux, *J. Am. Chem. Soc.*, **121**, 5581 (1999).

28 E. Coronado, J. R. Galan-Mascaros, C. J. Gomez-Garcia, and V. Laukhin, *Nature*, **408**, 447 (2000).

29 H. Fujiwara, E. Fujiwara, Y. Nakazawa, B. Z. Narymbetov, K. Kato, H. Kobayashi, A. Kobayashi, M. Tokumoto, and P. Cassoux, *J. Am. Chem. Soc.*, **123**, 306 (2001).

30 L. Martin, S. S. Turner, P. Day, P. Guionneau, J. K. Howard, D. E. Hibbs, M. E. Light, M. B. Hursthouse, M. Uruichi, and K. Yakusi, *Inorg. Chem.*, **40**, 1363 (2001), and references are cited therein.

31 T. Matsumoto, T. Sugimoto, H. Aruga-Katori, S. Noguchi, and T. Ishida, *Inorg. Chem.*, **43**, 3780 (2004).

32 D. E. Williams, *Acta Crystallogr., Sect. B*, **29**, 96 (1975).

33 S. Nakatsuji, A. Kitamura, A. Takai, K. Nishikawa, Y. Morimoto, H. Yasuoka, H. Kawamura, and H. Anzai, *Z. Naturforsch., B: Chem. Sci.*, **53**, 495 (1998).

34 O. Lindqvist, L. Anderson, J. Sieler, G. Steimecke, and E. Hoyer, *Acta Chem. Scand., Ser. A*, **36**, 855 (1982).

35 G. R. Luckhurst, "Spin Labeling: Theory and Applications," ed by L. J. Berliner, Academic Press, New York (1976), Chap. 4, particularly Fig. 4 and Eq. 49.

36 G. V. Rubenacker, J. E. Drumheller, K. Emerson, and R. D. Willet, *J. Magn. Magn. Mater.*, **54**, 1483 (1986).

37 J. C. Bonner and M. E. Fisher, *Phys. Rev.*, **135**, A640 (1964).

38 Y. Tomkiewicz, A. R. Taranko, and J. B. Torrance, *Phys. Rev. Lett.*, **36**, 751 (1976).

39 J. C. Bonner, H. W. J. Blote, J. W. Bray, and I. S. Jacobs, *J. Appl. Phys.*, **50**, 1810 (1979).